TECHNICAL NOTES

Mixed convection along slender vertical cylinders with variable surface heat flux

H. KHOUAJA, T. S. CHEN and B. F. ARMALY

Department of Mechanical and Aerospace Engineering and Engineering Mechanics,
University of Missouri–Rolla, Rolla, MO 65401, U.S.A.

INTRODUCTION

HEAT TRANSFER from heated cylinders is encountered in various applications, such as heat exchangers, cooling systems and electronic equipment. The buoyancy force induced by the heated surface affects considerably the heat transfer rate by either assisting or opposing the forced flow. This effect becomes particularly significant when the flow velocities are relatively low and the temperature difference between the surface and the free stream is high. The problem of mixed convection along vertical cylinders and needles has not been studied as extensively as the flat plate case. The results that have been reported for mixed convection along vertical cylinders do not include the case of variable heat flux at the surface.

The effect of buoyancy forces on forced convection along vertical cylinders was first analyzed by Chen and Mucoglu [1, 2]. They utilized the local nonsimilarity method to obtain solutions for the cases of uniform wall temperature (UWT) and uniform surface heat flux (UHF). Their results were restricted to a surface curvature parameter, defined as $\Lambda_F = 2(x/r_0)Re_x^{-1/2}$, from 0 to 8 and for Prandtl numbers of 0.7 and 7. Bui and Cebeci [3] solved the same problem using a finite-difference technique and presented results for the UWT case, for Prandtl numbers of 0.1, 1.0 and 10, and for curvature parameter Λ_F of up to 10. Later, S. L. Lee *et al.* [4, 5] extended the previous investigations of mixed convection along slender vertical cylinders to cover the entire regime, from pure forced convection to pure free convection, and presented results for a higher range of surface curvature parameter, $0 \leqslant \Lambda \leqslant 50$, where $\Lambda = 2(x/r_0)(Re_x^{1/2}+Gr_x^{1/4})^{-1}$ for the UWT case and $\Lambda = 2(x/r_0)(Re_x^{1/2}+Gr_x^{*1/5})^{-1}$ for the UHF case. They employed the weighted finite-difference method of solution [6] and their numerical results deviated from the ones reported by Bui and Cebeci, especially at large curvature parameters. This deviation was attributed to the inaccuracy from the use of the central finite-difference method of solution by Bui and Cebeci [3], which has difficulty handling the governing system of equations as they become 'stiff' when values of the surface curvature and Prandtl numbers become large.

Recently, H. R. Lee *et al.* [7] also employed the weighted finite-difference method to analyze natural convection along vertical cylinders for the case of power-law variation in the wall temperature, $T_w = T_\infty + ax^n$. They found that the previous results of S. L. Lee *et al.* [4] were not accurate for a curvature parameter Λ_N greater than 10, where $\Lambda_N = 2(x/r_0)Gr_x^{-1/4}$. This inaccuracy is attributed to the improper choice of step size in the radial direction η. More recently, Heckel *et al.* [8] extended the work of H. R. Lee *et al.* [7] to the case of power-law variation in the surface heat flux, $q_w(x) = ax^n$. A smaller step size and a larger value of

η_∞ were again used to obtain accurate results for the Nusselt number at high values of the curvature parameter. Heckel *et al.* [9] also analyzed the problem of mixed convection along slender vertical cylinders with a power-law variation in the wall temperature for the entire regime ranging from pure forced convection to pure free convection. Nusselt number results for higher values of the surface curvature were reported.

The present study is a supplement to the work of Heckel *et al.* [9] and deals with mixed convection along slender vertical cylinders for the case of variable surface heat flux $q_w(x) = ax^n$. No analytical results for this problem have been reported for the entire mixed convection regime except for the case of uniform surface heat flux (UHF, $n = 0$) [5]. The Nusselt number results are correlated using the correlation equation proposed by Churchill [10], $Nu^m = Nu_N^m + Nu_F^m$, where Nu_N is the local Nusselt number for pure free convection and Nu_F the local Nusselt number for pure forced convection.

ANALYSIS

Consider a long vertical cylinder of radius r_0 that is aligned parallel to a uniform, laminar free stream with velocity u_∞ and temperature T_∞. The surface of the cylinder is maintained at a variable heat flux $q_w(x)$. Let u and v represent the velocity components in the axial (x) and radial (r) directions, respectively, and T the fluid temperature. The conservation equations for the problem can be written as

$$\frac{\partial}{\partial x}(ru) + \frac{\partial}{\partial r}(rv) = 0 \tag{1}$$

$$u\frac{\partial u}{\partial x} + v\frac{\partial u}{\partial r} = \frac{v}{r}\frac{\partial}{\partial r}\left(r\frac{\partial u}{\partial r}\right) \pm g\beta(T - T_\infty) \tag{2}$$

$$u\frac{\partial T}{\partial x} + v\frac{\partial T}{\partial r} = \frac{\alpha}{r}\frac{\partial}{\partial r}\left(r\frac{\partial T}{\partial r}\right). \tag{3}$$

The boundary conditions are

$$u(x, r_0) = v(x, r_0) = 0, \quad \frac{\partial T}{\partial r}(x, r_0) = -\frac{q_w(x)}{k} \tag{4}$$

$$u(x, \infty) = u_\infty, \quad T(x, \infty) = T_\infty \tag{5}$$

$$u(0, r) = u_\infty, \quad T(0, r) = T_\infty, \quad \text{for } r \geqslant r_0. \tag{6}$$

In the above equations, a laminar boundary layer flow is assumed along with the Boussinesq approximation. The positive and negative signs in equation (2) correspond to upward and downward forced flows, respectively. In writing equation (6) the flow and the boundary layer thicknesses are assumed to be zero at the leading edge of the cylinder.

The governing equations (1)–(6) are first transformed into a dimensionless form by introducing the following dimensionless variables:

$$\eta = \frac{(r^2 - r_0^2)}{2r_0 x}(Re_x^{1/2} + Gr_x^{*1.5}),$$

$$\xi = [(x/r_0)/Re_0]^{1/4} \tag{7}$$

$$f(\xi, \eta) = \psi/[vr_0(Re_x^{1/2} + Gr_x^{*1/5})],$$

$$\theta(\xi, \eta) = (T - T_r)(Re_x^{1/2} + Gr_x^{*1.5})/[q_w(x)x/k] \tag{8}$$

$$\chi = (1 + \Omega_x^{1/5})^{-1}, \quad \Omega_x = Gr_x^*/Re_x^{5/2} \tag{9}$$

$$Gr_x^* = \frac{g\beta q_w(x)x^4}{kv^2}, \quad Re_x = \frac{u_x x}{v}, \quad Re_0 = \frac{u_\infty r_0}{v}. \tag{10}$$

In equation (8), $\psi(x, r)$ is the stream function that satisfies the continuity equation, with $u = (\partial\psi/\partial r)/r$ and $v = -(\partial\psi/\partial x)/r$. The buoyancy parameter Ω_x varies from zero to infinity. The limiting case of $\Omega_x = \infty$ corresponds to pure free convection along a vertical cylinder ($u_\infty = 0$) and mixed convection along a vertical flat plate ($r_0 = \infty$). The case of $\Omega_x = 0$ corresponds to pure forced convection. The mixed convection parameter χ varies from zero for pure free convection to one for pure forced convection.

The transformation yields

$$(1 + \eta\Lambda)f''' + \Lambda f'' + \tfrac{1}{10}[5 + (1-\chi)(2\gamma+3)]ff''$$
$$- \tfrac{1}{5}(1-\chi)(2\gamma+3)f'^2 \pm (1-\chi)^5\theta$$
$$= -\tfrac{1}{4}\xi\left(f''\frac{\partial f}{\partial\xi} - f'\frac{\partial f'}{\partial\xi}\right) \tag{11}$$

$$(1 + \eta\Lambda)\theta'' + \Lambda\theta' + \frac{Pr}{10}[5 + (1-\chi)(2\gamma+3)]f\theta'$$
$$- \frac{Pr}{10}[5 - (1-\chi)(2\gamma+3) + 10\gamma]f'\theta$$
$$= -\tfrac{1}{4}Pr\,\xi\left(\theta'\frac{\partial f}{\partial\xi} - f'\frac{\partial\theta}{\partial\xi}\right) \tag{12}$$

$$f(\xi, 0) = f'(\xi, 0) = 0, \quad \theta'(\xi, 0) = -1$$
$$f'(\xi, \infty) = \chi^2, \quad \theta(\xi, \infty) = 0 \tag{13}$$

where Λ is the curvature parameter defined as

$$\Lambda = 2\frac{x}{r_0}(Re_x^{1/2} + Gr_x^{*1.5})^{-1} \tag{14}$$

and

$$\gamma = \frac{x}{q_w}\frac{dq_w}{dx}. \tag{15}$$

For the case of power-law variation in surface heat flux, $q_w(x) = ax^n$, one has

$$\gamma = n. \tag{16}$$

The x-dependent parameter $\chi(x)$ and $\Lambda(x)$ can be related to the x-dependent $\xi(x)$ parameter such that

$$\Lambda = 2\xi^2\chi, \quad \chi = [1 + \Omega_0\xi^{(6+4n)/5}]^{-1} \tag{17}$$

where

$$\Omega_0 = [Gr_0^*/Re_0^{1-n}]^{1/5} \tag{18}$$

with $Gr_0^* = g\beta q_w(r_0)r_0^4/kv^2$ and $Re_0 = u_\infty r_0/v$ as before.

Equations (11) and (12) can be rewritten in a general form as

$$(1 + a_1\eta)f''' + a_1 f'' + a_2 ff'' + a_3 f'^2 + a_4\theta$$
$$= a_5\left(f'\frac{\partial f}{\partial\xi} - f'\frac{\partial f'}{\partial\xi}\right) \tag{19}$$

$$(1 + a_1\eta)\theta'' + a_1\theta' + Pr\,a_2 f\theta' + Pr\,a_6 f'\theta$$
$$= Pr\,a_5\left(\theta'\frac{\partial f}{\partial\xi} - f'\frac{\partial\theta}{\partial\xi}\right) \tag{20}$$

where

$$a_1 = \Lambda, \quad a_2 = \tfrac{1}{10}[5 + (1-\chi)(2n+3)],$$
$$a_3 = -\tfrac{1}{5}(1-\chi)(2n+3), \quad a_4 = \pm(1-\chi)^5, \quad a_5 = -\xi/4,$$
$$a_6 = -\tfrac{1}{10}[5 - (1-\chi)(2n+3) + 10n]. \tag{21}$$

With Λ and χ related to ξ and Ω_0, the functions f and θ in equations (11) and (12) or equations (19) and (20) are functions of (ξ, η) and depend on three constant parameters, n, Pr and Ω_0. One can then obtain solutions of equations (19) and (20) subject to boundary conditions (13) for all three cases, vertical cylinders in mixed convection ($u_\infty \neq 0$, $\Omega_0 = $ finite), vertical cylinders in pure free convection ($u_\infty = 0$, $\Omega_0 = \infty$), and vertical flat plates ($r_0 \to \infty$) in mixed convection ($\Omega_0 = \infty$, $\Lambda = 0$). The case of pure free convection along vertical cylinders has already been studied in details by Heckel et al. [8]. The limiting case of $r_0 = \infty$ for a flat plate with variable surface heat flux is solved in this particular study for comparison purposes. For the flat plate case, f and θ become functions of (χ, η) and equations (19) and (20) along with boundary conditions (13) still apply except that for this case ξ is replaced with χ and

$$\eta = \frac{y}{x}(Re_x^{1/2} + Gr_x^{*1/5}), \quad a_1 = \Lambda = 0,$$

$$a_5 = \frac{\chi}{10}(1-\chi)(3+2n) \tag{22}$$

with $y = r - r_0$.

The physical quantities of interest include the local and average Nusselt numbers, the local and average friction factors, the axial velocity distribution, and the temperature profile.

The local Nusselt number is defined by $Nu_x = [q_w/(T_w - T_\infty)](x/k)$, which can be expressed as

$$Nu_x/(Re_x^{1/2} + Gr_x^{*1/5}) = \frac{1}{\theta(\xi, 0)} \tag{23}$$

and the average Nusselt number is obtained from the expression

$$\overline{Nu_L}/(Re_L^{1/2} + Gr_L^{*1/5}) = 4\chi_L\xi_L^{-2}\int_0^{\xi_L}\frac{1}{\theta(\xi, 0)\chi}\xi\,d\xi \tag{24}$$

where $\xi_L = \xi$ at $x = L$. The local friction factor is obtained from the definition $C_{fx} = \tau_w/(\rho u_\infty^2/2)$, with $\tau_w = \mu(\partial u/\partial r)_{r0}$. This gives

$$C_{fx}Re_x^{1/2} = 2\chi^{-3}f''(\xi, 0). \tag{25}$$

The expression for the average friction factor is given by

$$\overline{C_{fL}}Re_L^{1/2} = 8\xi_L^{-2}\int_0^{\xi_L}\chi^{-3}f''(\xi, 0)\xi\,d\xi. \tag{26}$$

The axial velocity distribution can be written as $u/u_\infty = f'(\xi, \eta)/\chi^2$ and the temperature profile is given by

$$\theta(\xi, \eta) = (T - T_\infty)(Re_x^{1/2} + Gr_x^{*1/5})/[q_w(x)x/k]$$

or by

$$(T - T_x)/(T_w - T_\infty) = \theta(\xi, \eta)/\theta(\xi, 0).$$

METHOD OF SOLUTION

Equations (11)–(13) or (19), (20), and (13) constitute a system of non-linear partial differential equations in the (ξ, η) coordinates with parameters Pr, n and Ω_0. The major steps

Table 1. The $Nu_x Re_x^{-1/2}$ and $f''(\xi, 0)$ results for power-law variation in surface heat flux, forced convection

| | $Pr = 0.1$ | | | $Pr = 0.7$ | | | $Pr = 7$ | | | $Pr = 100$ | | | |
| | n | | | n | | | n | | | n | | | |
ξ	-0.4	0	0.5	-0.4	0	0.5	-0.4	0	0.5	-0.4	0	0.5	$f''(\xi, 0)$
0	0.1550	0.2007	0.2410	0.3209	0.4059	0.4803	0.7056	0.8856	1.0436	1.7165	2.1522	2.5349	0.3321
0.5	0.2470	0.3062	0.3562	0.4345	0.5385	0.6274	0.8662	1.0786	1.2627	1.9974	2.5014	2.9415	0.4797
1.0	0.4761	0.5585	0.6256	0.7044	0.8457	0.9620	1.2268	1.4997	1.7308	2.5690	3.1927	3.7308	0.8064
1.5	0.8297	0.9192	0.9979	1.0765	1.2617	1.4099	1.7075	2.0489	2.3316	3.2743	4.0257	4.6653	1.2387
2.0	1.3320	1.4078	1.4831	1.5381	1.7686	1.9506	2.2864	2.7013	3.0387	4.0866	4.9692	5.7110	1.7580
2.5	1.9509	2.0128	2.0806	2.0841	2.3670	2.5814	2.9555	3.4488	3.8441	5.0015	6.0199	6.8660	2.3579
3.0	2.6706	2.7235	2.7847	2.7154	3.0415	3.2952	3.7091	4.2853	4.7414	6.0142	7.1728	8.1253	3.0406
3.5	3.4880	3.5357	3.5920	3.4619	3.8042	4.0844	4.5422	5.2056	5.7254	7.1184	8.4211	9.4821	3.8166
4.0	4.4055	4.4496	4.5023	4.3357	4.6778	4.9717	5.4587	6.2152	6.8028	8.3214	9.7763	10.951	4.6973
4.5	5.4269	5.4684	5.5185	5.3364	5.6671	5.9683	6.4635	7.3201	7.9805	9.6329	11.249	12.545	5.6908
5.0	6.5597	6.5993	6.6474	6.4614	6.7763	7.0800	7.5611	8.5258	9.2646	11.056	12.847	14.271	6.8041

necessary to solve the non-linear system of equations are as follows. First, these equations are transformed into quasi-linear ordinary differential equations and are cast into a finite-difference form by making use of the weighting factors [6]. The resulting system of algebraic equations is next written in a matrix form that can be solved by the Gaussian elimination method with high accuracy. The solutions provide values for f, f' and θ, and the cubic spline technique is used to obtain the values of $f''(\xi, 0)$ and $\theta'(\xi, 0)$. A solution was considered to be convergent when the calculated values for f, f' and θ between two successive iterations differed by less than 10^{-4}.

The numerical solution was found to be very sensitive to the step size $\Delta\eta$ and the choice of η_∞. A step size of $\Delta\eta = 0.01$ and η_∞ values of up to 45 were used for all numerical calculations. These values were found to be sufficient for providing accurate results. A further decrease in $\Delta\eta$ or increase in η_∞ did not significantly affect the local Nusselt number results. In addition, it was found that the solution was not sensitive to the step size for $\Delta\xi$ and $\Delta\xi = 0.1$ was used.

RESULTS AND DISCUSSION

Numerical results were obtained for fluids with Prandtl numbers of 0.1, 0.7, 7 and 100, with the exponent n varying in the range $-0.4 \leqslant n \leqslant 0.5$, and for values of the buoyancy parameter Ω_0 of 0, 0.02, 0.1, 0.5, 1, 2 and ∞. The limiting case of $\Omega_0 = 0$ corresponds to pure forced convection along a vertical cylinder. The case of $\Omega_0 = \infty$ corresponds to either mixed convection along a vertical flat plate ($r_0 = \infty$) or to pure free convection ($u_\infty = 0$) along a vertical cylinder. The latter case has been studied in detail by Heckel et al. [8] and their results were used in this present study for developing the correlation equations.
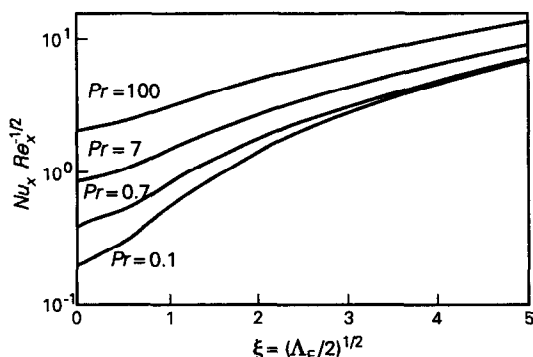
The local Nusselt number results $Nu_x Re_x^{-1/2}$ for pure forced convection ($\chi = 1$) are listed in Table 1. It can be seen from the table that the local Nusselt number increases with increasing Pr and n. Also, the local Nusselt number increases with increasing curvature (in terms of ξ) and seems to converge to an asymptotic value for high values of the curvature parameter $\Lambda_F = 2\xi^2$. This can be noticed from Fig. 1 which shows the local Nusselt number $Nu_x Re_x^{-1/2}$ as a function of ξ. The curves for all Pr merge together for high values of curvature Λ_F. The results of S. L. Lee et al. [5] for the UHF case are in agreement with the present results for small values of the curvature parameter Λ_F, but both sets of results deviate from each other for large values of Λ_F. For instance, for the case of $Pr = 0.7$ and $n = 0$ (UHF) the value of $Nu_x Re_x^{-1/2}$ was found to be 6.77 for $\Lambda_F = 50$ ($\xi = 5$) as compared to 16.5 as reported by S. L. Lee et al. [5]. The results for $f''(\xi, 0)$ are also included in Table 1. For the pure forced convection case, $f''(\xi, 0)$ is independent of Pr and n since for this case the energy equation is not coupled with the momentum equation.

Figure 2 demonstrates the effect of surface curvature parameter Λ_F on the local Nusselt number. As the figure illustrates, the local Nusselt number ratio $Nu_x/Nu_{x,p}$, where $Nu_{x,p}$ is the local Nusselt number for a vertical plate ($\Lambda_F = 0$), increases from 1 at $\Lambda_F = 0$ and is more sensitive to Λ_F for lower Prandtl numbers. To conserve space, results for the average Nusselt number $\overline{Nu_L}$ and for the $Nu_x/Nu_{x,UHF}$ ratio are not shown. The ratio $Nu_x/Nu_{x,UHF}$ tends to 1.0 for high curvature values, which indicates that the Nusselt number becomes independent of n as the curvature increases.

Numerical results for mixed convection are presented next. Table 2 presents the results for the local Nusselt number $Nu_x/(Re_x^{1/2} + Gr_x^{*1/5})$ for the limiting case of mixed convection over a vertical flat plate ($\Lambda = 0$ and $\Omega_0 = \infty$). The local

FIG. 1. $Nu_x Re_x^{-1/2}$ vs ξ for pure forced convection, UHF.
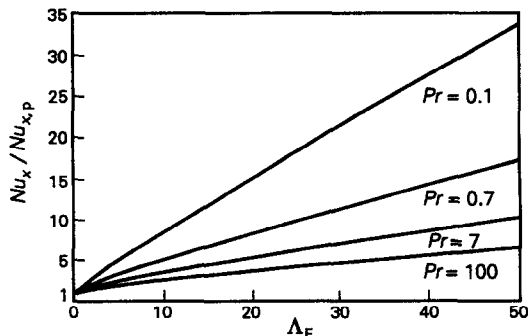
FIG. 2. $Nu_x/Nu_{x,p}$ vs Λ_F for pure forced convection, UHF.

Table 2. The $Nu_x/(Re_x^{1/2}+Gr_x^{*1/5})$ results for power-law variation in surface heat flux, mixed convection along a vertical flat plate ($\Lambda = 0, \Omega_0 = \infty$)

| | Pr = 0.1 | | | Pr = 0.7 | | | Pr = 7 | | | Pr = 100 | | |
| | | n | | | n | | | n | | | n | |
χ	−0.4	0	0.5	−0.4	0	0.5	−0.4	0	0.5	−0.4	0	0.5
0	0.2115	0.2635	0.3053	0.3975	0.4834	0.5517	0.7291	0.8699	0.9816	1.3134	1.5564	1.7493
0.1	0.1906	0.2374	0.2751	0.3583	0.4357	0.4972	0.6572	0.7841	0.8849	1.1841	1.4034	1.5775
0.2	0.1704	0.2122	0.2457	0.3206	0.3897	0.4446	0.5880	0.7017	0.7912	1.0629	1.2608	1.4180
0.3	0.1513	0.1882	0.2178	0.2851	0.3463	0.3948	0.5240	0.6255	0.7066	0.9616	1.1435	1.2910
0.4	0.1338	0.1664	0.1925	0.2531	0.3072	0.3515	0.4699	0.5625	0.6411	0.9015	1.0830	1.2490
0.5	0.1192	0.1485	0.1743	0.2275	0.2784	0.3237	0.4360	0.5322	0.6229	0.9177	1.1416	1.3687
0.6	0.1102	0.1413	0.1696	0.2168	0.2745	0.3251	0.4459	0.5679	0.6764	1.0388	1.3407	1.6085
0.7	0.1144	0.1504	0.1815	0.2356	0.3021	0.3588	0.5126	0.6538	0.7744	1.2406	1.5834	1.8762
0.8	0.1302	0.1697	0.2041	0.2700	0.3431	0.4066	0.5935	0.7482	0.8829	1.4431	1.8177	2.1440
0.9	0.1432	0.1856	0.2230	0.2965	0.3754	0.4444	0.6521	0.8190	0.9655	1.5862	1.9903	2.3451
1.0	0.1550	0.2007	0.2410	0.3209	0.4059	0.4803	0.7056	0.8856	1.0436	1.7165	2.1522	2.5349

Nusselt number results as a function of χ for the UHF ($n = 0$) case are illustrated in Figs. 3 and 4, respectively for $Pr = 0.7$ and 7.0. These figures cover the entire regime of mixed convection ($0 \leqslant \chi \leqslant 1$) with Ω_0 and Λ as parameters. Curves with constant values of Λ are also presented by dashed lines in the figures. The curves for $\Omega_0 = 0$ are for pure forced convection and the curves for $\Omega_0 = \infty$ cover both mixed convection along a vertical flat plate ($r_0 = \infty$ and $\Lambda = 0$) and pure free convection ($u_\infty = 0$ and $\chi = 0$) along a vertical cylinder. It can be seen from Figs. 3 and 4 how the local Nusselt number varies with χ for different values of Ω_0 and Λ. One can notice that for high values of Ω_0 the Nusselt number parameter $Nu_x/(Re_x^{1/2} + Gr_x^{*1/5})$ decreases from $\chi = 1$ (pure forced convection) to reach a minimum value near $\chi = 0.55$ and then increases toward $\chi = 0$ (pure free convection). However, this is not the behavior for the local

Nusselt number Nu_x. For example, for $\chi = 0.6$ and $Re_x^{1/2} = 100$, one has $Gr_x^{*1/5} = 66.67$ from equation (9). Next, from Table 2 one finds for the case of $Pr = 0.7$ and $n = 0$, $Nu_x Gr_x^{*-1/5} = 0.4834$ for pure free convection ($\chi = 0$), $Nu_x Re_x^{-1/2} = 0.4059$ for pure forced convection ($\chi = 1$), and $Nu_x(Re_x^{1/2} + Gr_x^{*1/5})^{-1} = 0.2745$ for mixed convection with $\chi = 0.6$. The corresponding local Nusselt numbers Nu_x for free convection, forced convection, and mixed convection are, respectively, 32.23, 40.59 and 45.75. This trend in the Nu_x values for the three convection regimes agrees with physical reasoning.

The effect of the exponent n on the local Nusselt number is illustrated in Fig. 5. The flat plate case with $Pr = 0.7$ is shown in the figure as an example. It is seen from the figure that the local Nusselt number increases with increasing n and that all curves approximately follow the same pattern as the UHF case ($n = 0$).

Results for $f''(\xi, 0)$ and the average Nusselt number results $\overline{Nu}_L/(Re_L^{1/2} + Gr_L^{*1/5})$ were also obtained for the mixed convection case, but they are not included to conserve space. The general trend for $f''(\xi, 0)$ results is that it decreases with increasing Prandtl number and increasing n, which is opposite to the Nusselt number behavior. The average Nusselt number results exhibit a similar behavior as the local Nusselt number.

For practical purposes, the local and average Nusselt number results for pure forced convection within the ranges $0.1 \leqslant Pr \leqslant 100$ and $-0.4 \leqslant n \leqslant 0.5$ have been correlated by the following expressions:

$$Nu_x Re_x^{-1/2} = \alpha_F(Pr)[A_F(\Lambda) + f_{1,F}(Pr)\Lambda](1 + V_F W_F) \quad (27)$$

where

$$\alpha_F(Pr) = 0.464 Pr^{1/3}[1 + (0.0207/Pr)^{2/3}]^{-1/4} \quad (28)$$
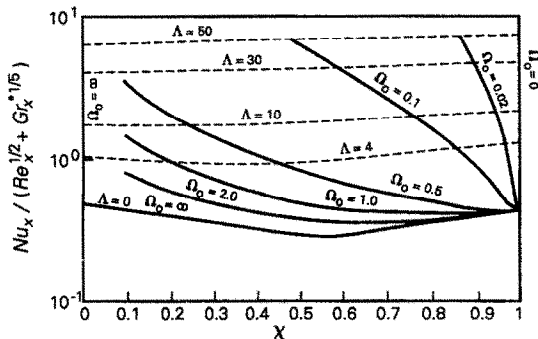
FIG. 3. $Nu_x/(Re_x^{1/2} + Gr_x^{*1/5})$ vs χ for mixed convection, $Pr = 0.7$, UHF.
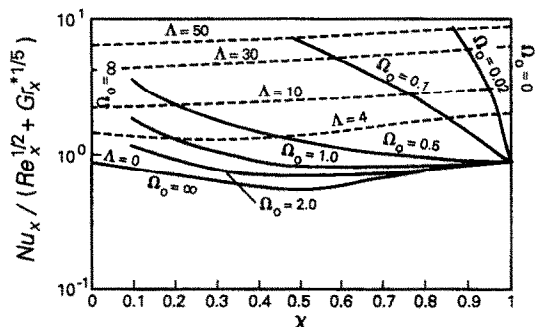
FIG. 4. $Nu_x/(Re_x^{1/2} + Gr_x^{*1/5})$ vs χ for mixed convection, $Pr = 7$, UHF.
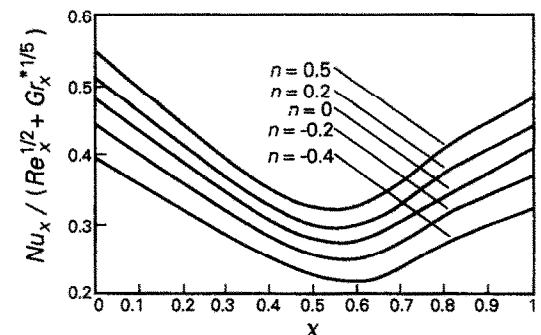
FIG. 5. $Nu_x/(Re_x^{1/2} + Gr_x^{*1/5})$ vs χ for mixed convection, $Pr = 0.7$, $\Lambda = 0$ (flat plate).

$$A_F(\Lambda) = 1 + 0.31\Lambda^{1/2} \tag{29}$$

$$f_{1,F}(Pr) = 0.015 + 0.24Pr^{-0.38} \tag{30}$$

$$V_F = n\{[0.44 + 5.0\exp(-6.0Pr^{1/10})] - 0.18n\} \tag{31}$$

$$W_F = \exp[-(0.06 + 0.1Pr^{-0.3})\Lambda^{3/5}]. \tag{32}$$

The corresponding expression for the average Nusselt number is

$$\overline{Nu}_L Re_L^{-1/2} = 2\alpha_F(Pr)[B_F(\Lambda) + f_{2,F}(Pr)\Lambda](1 + \bar{V}_F) \tag{33}$$

where

$$B_F(\Lambda) = 1 + 0.19\Lambda^{1/2} \tag{34}$$

$$f_{2,F}(Pr) = 0.012 + 0.12Pr^{-0.38} \tag{35}$$

$$\bar{V}_F = V_F \exp[-(0.08Pr^{-1/5})\Lambda^{0.70}]. \tag{36}$$

The form of the above correlation equations is similar to the one proposed by Heckel et al. [9]. Their form was based on the flat plate solution and the nearly linear relationship between the Nusselt number and the curvature. On the other hand, the correlations of S. L. Lee et al. [5] were derived based on the asymptotic solution as $\Lambda \to \infty$. The maximum error in equations (27) and (33) is less than 7.3% for the UHF case and increases to 10.1% for the variable heat flux case with $-0.4 \leqslant n \leqslant 0.5$. The maximum error occurs at $Pr = 0.1$ and $n = -0.4$.

In the entire mixed convection regime $0 \leqslant \chi \leqslant 1$, the correlation equations for Nusselt numbers can be presented in the form as proposed by Churchill [10]

$$(Nu/Nu_F)^m = 1 + (Nu_N/Nu_F)^m. \tag{37}$$

This form of correlation is based on pure forced and pure free convection results for a vertical flat plate. In terms of the buoyancy parameter χ the corresponding correlation equation can be represented by

$$Nu_x/(Re_x^{1/2} + Gr_x^{*1/5}) = \{[\chi(Nu_x Re_x^{-1/2})]^m + [(1-\chi)(Nu_x Gr_x^{*-1/5})]^m\}^{1/m}. \tag{38}$$

A correlation equation based on the graphical technique of Churchill was developed for the exponent m in terms of the curvature Λ and Pr as

$$m = 1 + 2\exp[-(0.75 + 0.40Pr^{-0.4})\Lambda^{0.3}]. \tag{39}$$

It is noted that the form of equation (39) is such that m tends to 3 for zero curvature ($\Lambda = 0$) which has been proven theoretically and experimentally to give good accuracy for the vertical flat plate case [10–12]. As Λ tends to infinity m decreases to 1. This can be explained by the Nusselt number being nearly independent of the buoyancy parameter χ for large Λ values. The Nusselt number calculations for pure free convection Nu_N and pure forced convection Nu_F, which are used in equation (38), are based on Λ. They are calculated from the endpoints of the curves in the Nusselt number figures at $\chi = 0$ and 1 for lines of constant Λ for given Pr and n. The maximum error in equation (38) was found to be less than 5% for the flat plate case with $m = 3$. For $\Lambda > 0$, equation (38) along with the m expression produces a maximum error of 8% when interpolating from the calculated Nu_N and Nu_F values. Similar to what has been reported by Heckel et al. [9], the correlation gives good results only for $n \geqslant 0$, and it is inconsistent for $n < 0$.

CONCLUSIONS

Mixed convection in laminar boundary layer flow along slender vertical cylinders is studied for power-law variation in surface heat flux. Numerical results are obtained for the entire mixed convection regime ($0 \leqslant \chi \leqslant 1$) and local Nusselt number parameter in terms of $Nu_x/(Re_x^{1/2} + Gr_x^{*1/5})$ are presented for $0.1 \leqslant Pr \leqslant 100$ and $0 \leqslant \Lambda \leqslant 50$, with $-0.4 \leqslant n \leqslant 0.5$. Correlation equations for the local Nusselt number are also included. The Nusselt number and hence the local heat transfer rate are found to increase with increasing Prandtl number, increasing curvature, and increasing value of the exponent n. For the vertical flat plate case ($\Lambda = 0$) the local Nusselt number parameter initially decreases and then increases as χ varies between 1 and 0. As the curvature is increased, the local Nusselt number parameter becomes nearly independent of the mixed convection parameter χ and the constant Λ curves appear almost as straight lines. Results for the average Nusselt number $\overline{Nu}_L/(Re_L^{1/2} + Gr_L^{*1/5})$ and $f''(\xi, 0)$ are also discussed.

REFERENCES

1. T. S. Chen and A. Mucoglu, Buoyancy effects on forced convection along a vertical cylinder, J. Heat Transfer 97, 198–203 (1975).
2. A. Mucoglu and T. S. Chen, Buoyancy effects on forced convection along a vertical cylinder with uniform surface heat flux, J. Heat Transfer 98, 523–525 (1976).
3. M. N. Bui and T. Cebeci, Combined free and forced convection on vertical cylinders, J. Heat Transfer 107, 476–478 (1985).
4. S. L. Lee, T. S. Chen and B. F. Armaly, Mixed convection along isothermal vertical cylinders and needles, Proc. Eighth Int. Heat Transfer Conf., Vol. 3, pp. 1425–1432 (1986).
5. S. L. Lee, T. S. Chen and B. F. Armaly, Mixed convection along vertical cylinders and needles with uniform surface heat flux, J. Heat Transfer 110, 711–716 (1987).
6. S. L. Lee, T. S. Chen and B. F. Armaly, New finite difference solution methods for wave instability problems, Numer. Heat Transfer 10, 1–8 (1986).
7. H. R. Lee, T. S. Chen and B. F. Armaly, Natural convection along vertical cylinders with variable surface temperature, J. Heat Transfer 110, 103–108 (1988).
8. J. J. Heckel, T. S. Chen and B. F. Armaly, Natural convection along a vertical cylinder with variable surface heat flux, J. Heat Transfer 111, 1108–1111 (1989).
9. J. J. Heckel, T. S. Chen and B. F. Armaly, Mixed convection along a vertical cylinder with variable surface temperature, Int. J. Heat Mass Transfer 32, 1431–1441 (1989).
10. S. W. Churchill, A comprehensive correlating equation for laminar assisting, forced and free convection, A.I.Ch.E. Jl 23, 10–16 (1977).
11. T. S. Chen, B. F. Armaly and N. Ramachandran, Correlations for laminar mixed convection flows on vertical, inclined, and horizontal flat plates, J. Heat Transfer 108, 835–840 (1986).
12. T. S. Chen and B. F. Armaly, Mixed convection in external flow. In Handbook of Single-phase Convective Heat Transfer (Edited by S. Kakac, R. K. Shah and W. Aung), Chap. 14. Wiley, New York (1987).